

# Demonstrating highly symmetric single-mode, single-photon heralding efficiency in spontaneous parametric downconversion

Marcelo Da Cunha Pereira,<sup>1,2</sup> Francisco E Becerra,<sup>1</sup> Boris L Glebov,<sup>1</sup> Jingyun Fan,<sup>1,\*</sup>  
Sae Woo Nam,<sup>3</sup> and Alan Migdall<sup>1</sup>

<sup>1</sup>Joint Quantum Institute, National Institute of Standards and Technology and University of Maryland, 100 Bureau Drive, Mail Stop 8441, Gaithersburg, Maryland 20899, USA

<sup>2</sup>Departamento de Física, Universidade Federal de Minas Gerais, Caixa Postal 702, Belo Horizonte, Minas Gerais 30123-970, Brazil

<sup>3</sup>National Institute of Standards and Technology, 325 Broadway, Boulder, Colorado 80305, USA

\*Corresponding author: [jfan@nist.gov](mailto:jfan@nist.gov)

Received January 28, 2013; revised March 20, 2013; accepted March 28, 2013;  
posted April 11, 2013 (Doc. ID 184274); published May 6, 2013

We demonstrate a symmetric, single-spatial-mode, single-photon heralding efficiency of 84% for a type-II spontaneous parametric downconversion process. High-efficiency, single-spatial mode collection is key to enabling many quantum information processing and quantum metrology applications.

OCIS codes: (270.5585) Quantum information and processing; (190.4410) Nonlinear optics, parametric processes.  
<http://dx.doi.org/10.1364/OL.38.001609>

Entanglement lies at the heart of quantum mechanics, and one of its most important uses is to test Bell's inequality to further our understanding of reality and locality [1]. As most commonly implemented, this test is carried out by examining the correlation between a pair of entangled photons [2]. Although many tests have been made of Bell's inequality since the seminal works of the 1970s and 1980s [3–5], an unqualified result has yet to be achieved. One fundamental reason is that a significant fraction of photons generated in such tests are not detected during measurement. While the measured correlations are explained by quantum mechanics, and most believe that quantum mechanics is indeed the mechanism behind those correlations, the low measurement efficiency does open the possibility of a cleverly designed local-hidden-variable theory that could reproduce the observed correlations without having to resort to quantum mechanics [6,7]. To close the loophole using Bell's original scheme, an overall efficiency, from the generation to the detection of the photons, of at least 83% is required [1]. By taking advantage of nonmaximal entanglement, Eberhard was able to relax this efficiency requirement to 67% [8]. But even this more moderate efficiency requirement still represents an extremely difficult technical challenge and has only recently been achieved [9,10]. While this is sufficient for closing the detection loophole, many proposed quantum information applications have an additional requirement that the photons be in a single optical spatial mode. In this Letter, we report an experimental demonstration of symmetric, single-spatial-mode, single-photon heralding efficiency of 84% for a type-II spontaneous parametric downconversion (SPDC) process.

Photon pairs are typically produced via an SPDC process, in which a higher energy photon is consumed to create a pair of correlated lower energy photons. (These photons are referred to as signal and idler photons in this Letter and have horizontal (H) and vertical (V) polarization, respectively.) The relevant efficiencies are the signal and idler photon heralding efficiencies ( $\eta_s$  and  $\eta_i$ ),

defined as the probability of a signal (idler) photon being present in the single-mode optical collection fiber, conditioned on an idler (signal) photon being detected by a single-photon detector (SPD). Experimentally, this is given by the ratio of the number of detected two-photon coincidence events ( $C$ ) to the number of detected idler (signal) photons  $N_i(N_s)$  in a given time period, after correcting for the detection efficiency of the signal (idler) SPD  $\eta_s^{\text{SPD}}(\eta_i^{\text{SPD}})$ . Thus the signal and idler heralding efficiencies are given by  $\eta_s = C/(N_i \cdot \eta_i^{\text{SPD}})$  and  $\eta_i = C/(N_s \cdot \eta_s^{\text{SPD}})$ , respectively. While ideally the detection of a signal (idler) photon heralds the presence of its twin with a probability of 100%, inefficiency in the collection and detection of photons after their creation results in unheralded photons and heralding photons whose twin never arrives. In addition to these losses, the measurements are often further degraded by stray light in the system and detector dark counts. Recent theoretical studies suggest the possibility of collecting the twin photons into single-mode optical fibers with near-unit efficiency [11,12], and on the detection front, experimentalists have made significant advances, pushing photon detection efficiencies close to 100% [13–15]. Inspired by these advances, we have experimentally demonstrated a symmetric, single-spatial-mode, single-photon heralding efficiency of 84%, i.e., when a signal photon is detected by an SPD, the probability of its twin idler photon being present in the other single-mode optical fiber is 84% and vice versa. This high symmetric efficiency, in a single-spatial-mode configuration, helps pave the way for many important quantum information applications, such as the device-independent quantum key distribution [16–19], as well as facilitating many quantum metrology applications.

The experimental layout [Fig. 1(a)] employs a grating-stabilized diode laser emitting cw light at 405 nm with a linewidth of less than 200 MHz. The laser light passes through a single-mode (for  $\lambda = 405$  nm) optical fiber to ensure a good single spatial mode, a Glan–Taylor polarizer for a high degree of linear polarization, and a 10 nm

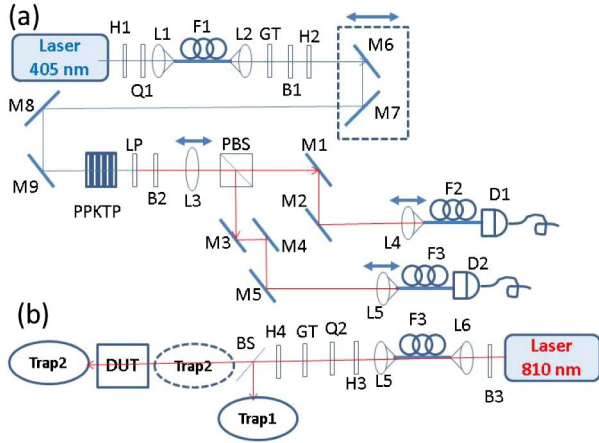


Fig. 1. (a) Complete optical setup of collinear type-II SPDC source and collection, (b) optical setup for calibrating transmittance of a device under test (DUT). Q1,  $\lambda/4$  plate at 405 nm; Q2,  $\lambda/4$  plate at 810 nm; H1 and H2,  $\lambda/2$  plates at 405 nm; H3 and H4,  $\lambda/2$  plates at 810 nm; L1 to L6, lenses. Focal lengths for L1 and L2:  $f = 14$  mm; and for L4 and L5:  $f = 11$  mm. Lenses with  $f = 300, 400, 500,$  and  $750$  mm were used for L3 to produce the collection beam waists of 60, 90, 120, and 175  $\mu\text{m}$  in Fig. 2 with appropriate adjustments in the optical path length. F1 to F3, single-mode optical fibers; GT, Glan-Taylor polarizer; B1 (B2), 10 nm bandpass filter centered at 405 nm (810nm); B3, 2 nm bandpass filter centered at 810 nm; LP, long pass filter ( $>600$  nm); M1 to M9, mirrors; PBS, polarizing beam splitter; BS, 50/50 nonpolarizing beam splitter; D1 and D2, SPDs. Arrows above some optical elements indicate that these elements are translated to produce the desired beam waist.

bandpass filter centered at 405 nm to eliminate light at longer wavelengths. A half-wave plate and a quarter-wave plate are used to adjust the optical power of the pump beam transmitted through the polarizer. A desired pump beam waist is set at the center of a 25 mm long periodically poled potassium titanyl phosphate (PPKTP) crystal by positioning a single aspheric lens (L2, with  $f = 14$  mm) and adjusting a variable length optical path. The crystal's cross section is 1 mm  $\times$  1 mm. A half-wave plate before the crystal is used to adjust the polarization of the pump beam to maximize the twin-photon yield of the SPDC. The PPKTP crystal is designed to convert  $H$ -polarized photons at 405 nm into pairs of orthogonally ( $H$ - and  $V$ -) polarized photons degenerate at 810 nm via type-II phase-matched SPDC. Immediately after the crystal are a long-pass filter ( $>600$  nm) and a 10 nm flat-top bandpass filter centered at 810 nm that together suppress the pump light by more than 150 dB. A collection lens (L3) is placed with its focus at the center of the crystal to nominally collimate the produced twin  $H$ - and  $V$ -polarized photons, which are separated using a polarizing beam splitter. Then aspheric lenses L4 and L5, one focal length from the fibers F2 and F3 (core diameter of 4.4  $\mu\text{m}$ , single mode for 810 nm light), collect the collimated light into the single-mode fibers, which are connected to SPDs (commercially available fiber-coupled silicon photon-counting modules).

The optical paths and modes of the signal and idler photons are defined by the light coupled into the single-mode optical fibers just before the SPDs. These optical paths and the pump beam are aligned to overlap at the center of the PPKTP crystal. Because high overall optical

efficiency is the goal of this effort, it is helpful to determine the transmittances of all the components in the optical path. To do this we sent an 810 nm laser polarized either horizontally or vertically backward through the system using the single-mode fiber in front of each SPD to ensure that we were measuring the transmittances of only the spatial mode of interest [Fig. 1(b)]. To monitor and correct for any drifts in the incident optical power, a 50/50 nonpolarizing beam splitter was used after the single-mode fiber to send half of the light to a high-spatial-uniformity, high-stability detector, a calibrated silicon photodiode trap (Trap1) [20]. The rest of the light went to the optical element [device under test (DUT)]. The optical power was measured before and after the DUT by a second-calibrated silicon photodiode trap (Trap2). The ratio of those measurements, after normalizing to the power measured by Trap1, yields the absolute transmittance of the DUT at 810 nm with high accuracy. The optical transmittance of the PPKTP crystal at 810 nm is measured in the same way, with the transmittance from the center of the crystal given by the square root of the total transmittance. The measured transmittances for horizontally and vertically polarized light at 810 nm of all optical elements in the beam path are summarized in Table 1. The SPDs were calibrated against the trap detector, and the efficiencies are also listed in Table 1. The optical loss of the antireflection coating on each end of the single-mode optical fiber is as quoted by the manufacturer.

In the determination of single-photon heralding efficiency, the UV pump beam was kept at 2.5 mW and the beam waist was 220  $\mu\text{m}$ . The single-photon detection rate at each SPD was 50,000 events per second or less. The FWHM of the spectrum of the photons collected into single-mode optical fibers was measured to be 0.2 nm. The single-photon, single-spatial-mode heralding efficiencies are shown in Fig. 2(a) as a function of the signal and idler collection beam waists (at the center of the crystal), with the highest efficiencies are being 84.4(5)% and 83.7(5)% for the idler and signal photons, respectively. [Corrections for background counts are 146(1)/s (242[1]/s) for the signal (idler) arm.] These are the highest such symmetric efficiencies reported to date (compare to previous results [11,21]). We measured the same heralding efficiencies to within 0.1% by varying the pump power

Table 1. Optical Transmittances<sup>a</sup>

Component	$T_H$ (Signal)	$T_V$ (Idler)
PPKTP	0.99280(4)	
LP	0.9918(1)	
B2	0.97976(5)	
L3	0.98558(6)	
PBS	0.982(1)	0.984(2)
M1 + M2	0.993(2)	
M3 + M4 + M5		0.993(2)
L4	0.9891(2)	
L5		0.9891(2)
F2, F3 (both ends)	0.997(2)	
Path <sup>b</sup>	0.914(3)	0.916(3)
SPD detection efficiency	0.504(5)	0.450(5)

<sup>a</sup>All uncertainties are 1 standard deviation.

<sup>b</sup>Product of measured transmittances of individual optical elements.

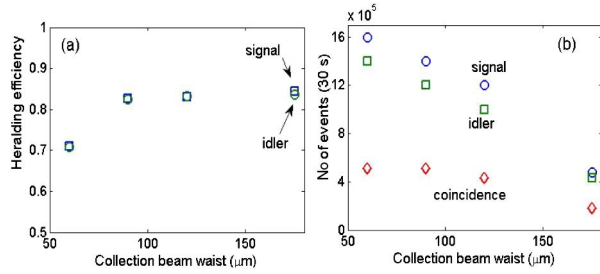


Fig. 2. (a) Heralding efficiencies as a function of the optical beam waist of the collection mode at the center of the crystal, corrected for SPD efficiencies and (b) detected single-photon and two-photon coincident events in 30 s.

continuously from 0.4 to 2.7 mW, indicating that any contribution from the multiple-photon-pair process is negligible ( $<0.1\%$  given the maximum detected count rate and the 5 ns coincidence window). Figure 2(b) shows the number of detections registered by the SPDs as a function of the collection beam waists. The corresponding efficiencies for collecting photons into the single-mode optical fibers, often referred to as mode-coupling efficiencies, were determined to be 92.1(6)% and 91.6(6)%, after correction for the optical transmittances listed in Table 1.

In conclusion, we have experimentally demonstrated a symmetric, single-spatial-mode, single-photon heralding efficiency of 84% in a type-II SPDC process. This high efficiency was achieved through improved mode matching, with the data pointing toward larger collection mode waists. The high efficiency along with the single-spatial-mode character demonstrated here promises a wide utility for research in fundamental physics and quantum information processing applications, and as a high water mark, it may spur the development of theoretical models of the SPDC process.

This research is partially supported by Physics Frontier Center at the Joint Quantum Institute. M. D. C. P. acknowledges support from the Brazilian funding agency FAPEMIG.

## References

1. J. S. Bell, *Physics* **1**, 195 (1964).
2. J. F. Clauser, M. A. Horne, A. Shimony, and R. A. Holt, *Phys. Rev. Lett.* **23**, 880 (1969).
3. S. J. Freedman and J. F. Clauser, *Phys. Rev. Lett.* **28**, 938 (1972).
4. E. S. Fry and R. C. Thompson, *Phys. Rev. Lett.* **37**, 465 (1976).
5. A. Aspect, P. Grangier, and G. Roger, *Phys. Rev. Lett.* **49**, 1804 (1982).
6. P. M. Pearle, *Phys. Rev. D* **2**, 1418 (1970).
7. A. Garg and N. D. Mermin, *Phys. Rev. D* **35**, 3831 (1987).
8. P. H. Eberhard, *Phys. Rev. A* **47**, R747 (1993).
9. M. Giustina, A. Mech, S. Ramelow, B. Wittmann, J. Kofler, A. Lita, B. Calkins, T. Gerrits, S. W. Nam, R. Ursin, and A. Zeilinger, "Bell violation with entangled photons, free of the fair-sampling assumption," <http://arxiv.org/abs/1212.0533> (2013).
10. S. Ramelow, A. Mech, M. Giustina, S. Groeblacher, W. Wieczorek, A. Lita, B. Calkins, T. Gerrits, S. W. Nam, A. Zeilinger, and R. Ursin, *Opt. Express* **21**, 6707 (2013).
11. D. Ljunggren and M. Tengner, *Phys. Rev. A* **72**, 062301 (2005).
12. R. S. Bennink, *Phys. Rev. A* **81**, 053805 (2010).
13. A. E. Lita, A. J. Miller, and S. W. Nam, *Opt. Express* **16**, 3032 (2008).
14. A. J. Miller, A. E. Lita, B. Calkins, I. Vayshenker, S. M. Gruber, and S. W. Nam, *Opt. Express* **19**, 9102 (2011).
15. D. Fukuda, G. Fujii, T. Numata, K. Amemiya, A. Yoshizawa, H. Tsuchida, H. Fujino, H. Ishii, T. Itatani, S. Inoue, and T. Zama, *Opt. Express* **19**, 870 (2011).
16. A. Acín, N. Brunner, N. Gisin, S. Massar, S. Pironio, and V. Scarani, *Phys. Rev. Lett.* **98**, 230501 (2007).
17. S. Pironio, A. Acín, N. Brunner, N. Gisin, S. Massar, and V. Scarani, *New J. Phys.* **11**, 045021 (2009).
18. C. Cyril Branciard, E. G. Cavalcanti, S. P. Walborn, V. Scarani, and H. M. Wiseman, *Phys. Rev. A* **85**, 010301 (2012).
19. M. Lucamarini, G. Vallone, I. Gianani, P. Mataloni, and G. Di Giuseppe, *Phys. Rev. A* **86**, 032325 (2012).
20. T. R. Gentile, J. M. Houston, and C. L. Cromer, *Appl. Opt.* **35**, 4392 (1996).
21. A. Fedrizzi, T. Herbst, A. Poppe, T. Jennewein, and A. Zeilinger, *Opt. Express* **15**, 15377 (2007).